Optimized Smoothing of GRACE Time-Variable Gravity Observations

J.L. Chen [1], C.R. Wilson [1,2], K.-W. Seo[3]

[1] Center for Space Research, University of Texas, Austin, TX 78712, USA
[2] Department of Geological Sciences, University of Texas, Austin, TX 78712, USA
[3]Jet Propulsion Laboratory, California Institute of Technology, Pasadena, CA 91109, USA

Contact Information:

Dr. Jianli Chen
Center for Space Research
3925 W. Braker Lane, Suite 200
Austin, TX 78759-5321, USA

Phone: 512-232-6218
Fax: 512-471-3570
Email: chen@csr.utexas.edu

Abstract:

High degree and order spherical harmonics of time-variable gravity fields observed by the Gravity Recovery and Climate Experiment (GRACE) gravity mission are dominated by noise. We develop two smoothing methods that suppress these high degree and order errors with results superior to more commonly used Gaussian smoothing. These optimized smoothing methods considerably improve signal-to-noise levels of GRACE terrestrial water storage estimates relative to residual signal and noise over the oceans, and show significantly better spatial resolution and lower leakage error. Based on analysis using an advanced land surface model, the equivalent spatial resolution from these optimized smoothing estimates is about 500 km, compared to roughly 800 – 1000 km Gaussian smoothing that is required to suppress high order errors in the GRACE fields.

Keywords. GRACE, Gravity, Gaussian, Smoothing, Water, Variance-Dependent

1. Introduction

The Gravity Recovery and Climate Experiment (GRACE) twin satellite gravity mission was launched in March 2002, with a primary goal to measure Earth's gravity and changes with respect to time [*Tapley et al*., 2004a]. GRACE time-variable gravity data are being used to infer mass load variations on the Earth surface [e.g., *Wahr et al.*, 1998, 2004; *Tapley et al*., 2004b]. However, variations in GRACE high degree Stokes coefficients are dominated by noise,

requiring spatial smoothing in order to derive useful measures of surface mass or geoid height changes [e.g., *Wahr et al.*, 1998; *Chen et al*., 2005a]. At global and basin scales, Gaussian smoothing [Jekeli, 1981] is commonly used to suppress high degree noise in GRACE fields [e.g., *Wahr et al*., 1998, 2004; *Tapley et al*., 2004b]. Gaussian smoothing is appropriate when the spatial distribution of noise is isotropic, because the operation corresponds to convolution over the Earth's surface with a circularly symmetric function. Although GRACE noise does not fully meet this assumption, when the effective radius of the smoothing is properly chosen (typically around 800 - 1000 km), GRACE terrestrial water storage changes agree fairly well with hydrological model estimates [e.g., *Wahr et al*., 2004; *Tapley et al*., 2004b; *Chen et al*., 2005a,b]. *Chambers et al*. (2004) and *Chen et al*. (2005c) demonstrate that with proper Gaussian smoothing, GRACE estimates of ocean mass variations agree remarkably well with non-steric global mean sea level changes derived from satellite altimeter observations.

Two main limitations of Gaussian smoothing are that 1) as effective radius increases, there is increased leakage error associated with a limited range of spherical harmonics, and 2) the Gaussian smoothing assigns isotropic weights in the spatial domain or only degree-dependent weights in spherical harmonics domain. These limit the utility of GRACE in the study of water storage in small river basins [*Swenson and Wahr*, 2002], though for the very largest basins this is less of a problem [*Wahr et al*., 2004; *Tapley et al*., 2004b; *Chen et al*., 2005b]. Errors in GRACE Stokes coefficients are related to the polar orbit ground tracks [*Tapley et al*., 2004b; *Chen et al*., 2005a], with a concentration at high orders, producing longitudinal stripes in

unsmoothed maps of load variation, which suggests that people will need a non-isotropic filter to more effectively remove these non-isotropic noise. A recent study by *Han et al* [2005a] recognizes the high-order noise, and employs order-depending (or no-isotropic) smoothing. However smoothing of any sort may also influence estimated signal. A recent study [*Chen et al*., 2005d] shows that Gaussian smoothing significantly affects basin-scale water storage estimates, even for the largest river basins. For example, with 1000 km Gaussian smoothing, seasonal magnitudes of GRACE water storage estimates in the Amazon and Mississippi are reduced about 35%, and the phase of the annual change is also affected. Thus, one must either account for these effects using independent data [e.g., *Chen et al*., 2005d] or develop another technique.

Basin functions are sets of coefficients used to form a linear combination of GRACE spherical harmonics to estimate water storage changes within a specific basin. Basin functions are designed using various criteria to maximize spatial resolution of the basin, and minimize effects of noise. *Swenson and Wahr* [2002] used a Lagrange multiplier method to optimize basin functions, using the full signal and error covariance matrices for azimuthally asymmetric basins. *Seo and Wilson* [2005] developed dynamic basin functions with time-variable weightings based on climate models, and showed that this method works well when good climate models are available. The dynamic basin function concept can also be applied to global-scales water storage estimates. An alternative approach to basin-scale water storage estimates was described by *Han et al.* (2005b) in which GRACE satellite-to-satellite tracking data are

used to directly estimate regional water storage change. This method bypasses intermediate steps of estimating spherical harmonic coefficients, and then linearly combining them using basin functions. GRACE satellite-satellite tracking data have recently become available in a public release, inviting more studies with this approach.

The objective of this study is to develop global optimized variance-dependent smoothing techniques to be used with GRACE time variable spherical harmonic coefficients. The goals are to more effectively reduce effects of high degree and order noise, to minimize attenuation of signal relative to conventional Gaussian smoothing, and to yield maximum signal-to-noise ratio (as defined later). We examine the variance spectrum of GRACE spherical harmonic Stokes coefficients as a function of degree and order, compare GRACE spectra with those of advanced climate models, and develop variance-dependent smoothing methods. Most atmospheric and barotropic oceanic mass redistribution effects have been removed from GRACE data in the GRACE dealiasing process [*Bettadpur*, 2003]. Thus GRACE data mainly reflect contributions from terrestrial water storage and snow/ice mass changes and the residual baroclinic signals over the oceans [Wahr et al., 2004], plus measurement errors and errors in the dealiasing (atmospheric, oceanic, tide) models. This is confirmed by the observation that, after reasonable smoothing, GRACE surface mass changes are dominated by the global hydrological cycle, with generally good agreement with major basin-scale water storage changes predicted by land surface models [e.g., *Wahr et al*., 2004; *Tapley et al*., 2004b; *Chen et al*., 2005a,b].

GRACE signal variance over land is (and should be) significantly higher than over the ocean, and this condition can be used to construct an optimized smoother, with a criterion of maximizing the ratio of variance over land relative to that over the oceans.

The following sections introduce the GRACE data and hydrological model used in this study, variance analysis of GRACE measurements and model estimates, construction of variance-dependent smoothing methods, optimization of these smoothing methods, and assessment through comparison with Gaussian smoothing and climate model estimates. A summary and general discussion is provided at the end.

2. Data and Processing

2.1 GRACE Time-Variable Gravity

We utilize the 22 GRACE monthly gravity field solutions for the period April 2002 to July 2004 from the release R001 [*Bettadpur*, 2003], consisting of fully normalized Stokes coefficients up to degree and order 120. The initial mean gravity field used is the GRACE GGM01 gravity model, derived from the first 111 days of GRACE data [*Tapley et al.,* 2004a]. Tidal effects, including ocean, solid Earth, and solid Earth pole tides (rotational deformation) have been removed in the level-2 GRACE data processing, and non-tidal atmospheric and oceanic contributions are also removed in the level-2 de-aliasing process (for details, see

Bettadpur, 2003). Consequently, GRACE time-variable gravity represents effects from geophysical phenomena not already modeled (mainly terrestrial water storage and snow/ice change), uncertainties in the *a priori* models, and errors in GRACE measurements. There are additional aliasing errors associated with the space-time sampling provided by the satellite ground track that is used to construct a nominal monthly mean gravity field.

2.2 Hydrological Model Estimate

Soil moisture and snow estimates are from NASA's Global Land Data Assimilation System (GLDAS) [*Rodell et al*., 2004]. GLDAS is an advanced land surface modeling system jointly developed by scientists at the NASA Goddard Space Flight Center (GSFC) and the NOAA National Centers for Environmental Prediction. GLDAS parameterizes, forces, and constrains sophisticated land surface models with ground and satellite products with the goal of estimating land surface states (e.g., soil moisture and temperature) and fluxes (e.g., evapotranspiration). In this particular simulation, GLDAS drove the Noah land surface model [*Ek et al*., 2003] version 2.7.1, with observed precipitation and solar radiation included as inputs. GLDAS estimates are the sum of soil moisture (2 m column depth) and snow water equivalent. Greenland and Antarctica are excluded because the Noah model does not include ice sheet physics. The GLDAS data are provided on 1° x 1° grids and at 3-hourly intervals.

GLDAS terrestrial water storage changes (soil moisture plus snow water) are expanded into fully normalized Stokes coefficients up to degree and order 100. Consistent with GRACE measurements, the degree-0 term (C_{00}), representing total water mass change, and degree-1

terms (C_{11}, S_{11}, C_{10}), representing geocenter motion [*Chen et al*., 1999] are excluded in GLDAS data, as these terms are not provided by GRACE. The degree-2 zonal term (C_{20}) is also removed from both GRACE and GLDAS data, because this term is thought to have large errors in the GRACE data (release R001). The 3-hourly GLDAS soil moisture and snow water data are averaged into the same GRACE 'monthly' intervals before further data processing.

To better resemble GRACE-observed surface mass changes, we also include the residual baroclinic oceanic mass variations using the differences of ocean bottom pressure estimates from two models. One is the Estimating the Circulation and Climate of the Ocean (ECCO) consortium's baroclinic data-assimilating ocean general circulation model, developed at NASA Jet Propulsion Laboratory, and the other is the same barotropic ocean general circulation model used in GRACE dealiasing process [*Bettadpur*, 2003]. These differential baroclinic oceanic mass changes are provided (with our great appreciation) by John Wahr at the University of Colorado, and are considered to represent the residual oceanic signals left in GRACE data [for details see Wahr et al., 2004].

2.3 Recovering Water Mass Change from GRACE and GLDAS

Global surface water mass change $\Delta\sigma$ can be computed from either GRACE or climate model Stokes coefficients as [*Wahr et al*., 1998],

$$\Delta\sigma(\theta,\phi) = \frac{R_E \rho_{ave}}{3} \sum_{l=0}^{N} \sum_{m=0}^{l} \frac{2l+1}{1+k_l} \tilde{P}_{lm}(\cos\theta) \times [\Delta C_{lm} \cos(m\phi) + \Delta S_{lm} \sin(m\phi)] \quad (1)$$

where R_E is the mean radius of the Earth, θ and ϕ are colatitude and east longitude, ΔC_{lm} and ΔS_{lm} are the fully normalized Stokes coefficients of degree l and order m, $\tilde{P}_{lm}$ are normalized associated Legendre functions, and k_l is the load Love number (of degree l). ρ_{ave} is the mean density of the Earth. When dealing with real data either from GRACE or model, the summation goes to a fixed degree (N).

GRACE high degree and order Stokes coefficients are dominated by noise, and equation (1) needs to be modified to account for this [e.g., *Chen et al.*, 2005a]. Using Gaussian smoothing [*Jekeli*, 1981] to suppress high degree and order terms equation (1) can be rewritten as [*Wahr et al.*, 1998],

$$\Delta\sigma(\theta,\phi) = \frac{R_E \rho_{ave}}{3} \sum_{l=0}^{N} \sum_{m=0}^{l} \frac{2l+1}{1+k_l} W_l \tilde{P}_{lm}(\cos\theta) \times [\Delta C_{lm} \cos(m\phi) + \Delta S_{lm} \sin(m\phi)] \quad (2)$$

where $W_l = W_l(r)$ is the normalized Gaussian weighting function (with maximum weight of 1), dependent on the selected effective radius (r). W_l reduces contributions from high degree and order Stokes coefficients, suppressing noise in the derived mass change fields. Gaussian smoothing gives equal weight W_l to all orders of Stokes coefficients at each degree (l), equivalent to convolution with a circular Gaussian shaped filter. Radius r corresponds to the distance at which the weight drops to half its peak value at the shortest wavelength [*Wahr et al.*, 1998].

Considering a non-isotropic filter, a more general format of eq. (2) is as following,

$$\Delta\sigma(\theta,\phi) = \frac{R_E \rho_{ave}}{3} \sum_{l=0}^{N} \sum_{m=0}^{l} \frac{2l+1}{1+k_l} \tilde{P}_{lm}(\cos\theta) \times [W_{lm}^{C} \Delta C_{lm} \cos(m\phi) + W_{lm}^{S} \Delta S_{lm} \sin(m\phi)] \quad (3)$$

where W_{lm}^{C} and W_{lm}^{S} represent the no-isotropic weights assigned for each Stokes coefficient. The focus of this study (and also of many previous studies as discussed earlier) is to find out how to define and determine the optimized weights for each Stokes coefficient.

3. Optimized Variance-Dependent Smoothing

High order GRACE Stokes coefficients tend to be dominated by noise, especially sectorial terms ($m=l$) [*Tapley et al*., 2004b; *Chen et al*., 2005a]. Gaussian smoothing sufficient to suppress this high order noise also attenuates signal in lower order Stokes coefficients (of the same degree). Two methods cited earlier, *Han et al.* [2005a] and *Seo and Wilson* [2005] address this problem in different ways. *Seo and Wilson* use the ratio of signal to signal plus noise variance at each degree and order, a least squares optimum weight. However, their approach requires knowledge of both signal and noise variance at each degree and order, which both may only be known approximately. *Han et al.* [2005a] use non-isotropic weighting with Gaussian-type operators that suppress high order terms. This is effective, but not a well-defined optimization strategy. Here we develop a new criterion based on maximizing the ratio of land variance to ocean variance in the estimates.

As a first step, we compute RMS deviations about the mean at each degree and order for the 22 GRACE solutions and GLDAS estimates. Next, we compute the ratio of GRACE to GLDAS RMS values. The RMS ratio, up to degree and order 60 is in Figure 1. We interpret a ratio much larger than 1 as evidence of a large noise level in the GRACE data at that degree and order.

Ratios are close to unity, up to about degree 20. Significant variations with degree and order are evident beyond this.

We construct two variance-dependent smoothing methods with adjustable parameters. The first is based on the RMS ratio (Figure 1) and we call this method RMS, with weights of the form,

$$W_{lm}^{C} = \left[\frac{RMS(C_{lm}^{MDL})}{RMS(C_{lm}^{GRC})} * a\right]^{b}, \quad when \quad W_{lm}^{C} > 1, \quad W_{lm}^{C} = 1$$
$$W_{lm}^{S} = \left[\frac{RMS(S_{lm}^{MLD})}{RMS(S_{lm}^{GRC})} * a\right]^{b}, \quad when \quad W_{lm}^{S} > 1, \quad W_{lm}^{S} = 1 \qquad (4)$$

in which, W_{lm}^{C} and W_{lm}^{S} are the assigned weights to the Stokes coefficients ΔC_{lm} and ΔS_{lm}. a and b are two variable scale factors. $RMS(C_{lm}^{MDL},\ S_{lm}^{MDL})$ and $RMS(C_{lm}^{GRC},\ S_{lm}^{GRC})$ are the RMS of coefficients from GRACE (abbreviated GRC) and GLDAS plus residuals over the oceans (abbreviated *MLD*). Parameters (*a, b*) are selected to maximize the ratio of variance over land areas, relative to the oceans, as discussed below. The maximum value of the weights (W_{lm}^{C} and W_{lm}^{S}) is 1. So, when W_{lm}^{C} or $W_{lm}^{S} > 1$, they are assigned to equal to 1 (the same is applied to eq. (5)).

The second smoothing method uses formal errors estimated and reported with GRACE Stokes coefficients [*Bettadpur*, 2003]. We call this method FM, and with weights of the form,

$$W_{lm}^{C} = \frac{RMS(C_{lm}^{MDL})^2}{RMS(C_{lm}^{MDL})^2 + (SIG(C_{lm}^{GRC}) * k)^2}, \quad when \quad W_{lm}^{C} > 1, \quad W_{lm}^{C} = 1$$
$$W_{lm}^{S} = \frac{RMS(S_{lm}^{MDL})^2}{RMS(S_{lm}^{MDL})^2 + (SIG(S_{lm}^{GRC}) * k)^2}, \quad when \quad W_{lm}^{S} > 1, \quad W_{lm}^{S} = 1 \qquad (5)$$

where $SIG(C_{lm}^{GRC},\ S_{lm}^{GRC})$ are the reported formal errors. These weights correspond to least squares optimum values, assuming that GLDAS results are the true signal. An alternative, examined by *Seo and Wilson* [2005] employed modified GRACE results as signal variance estimates. This changes the results only slightly. Because reported errors probably under-estimate true errors [*Wahr et al*., 2004], an adjustable scaling parameter (k) is included. *Seo and Wilson* [2005] used $k=5$, while here we search for a value that minimizes signal variance over the oceans, as described below.

We assume that GRACE measurement errors are approximately at the same level over both land and ocean. Then RMS GRACE estimates over land and oceans are the sum of the signal ($MASS_{land}$) and ($MASS_{ocean}$) plus noise (Err), so the ratio is

$$RMS\_Ratio = \frac{RMS(MASS_{land} + Err)}{RMS(MASS_{ocean} + Err)} \tag{6}$$

It is expected that $RMS(MASS_{land}) > RMS(MASS_{ocean})$, so for any ($Err$),

$$\begin{aligned} &\frac{RMS(MASS_{land})}{RMS(MASS_{ocean})} \geq RMS\_Ratio \geq 1, \quad and \\ &RMS\_Ratio = \frac{RMS(MASS_{land})}{RMS(MASS_{ocean})}, \quad when \quad Err = 0 \\ &RMS\_Ratio \approx 1, \quad when \quad RMS(Err) >> RMS(MASS_{land}) \end{aligned} \tag{7}$$

That is, for any given level of smoothing, RMS_Ratio falls between $\left[1,\ \frac{RMS(MASS_{land})}{RMS(MASS_{ocean})}\right]$. To optimize each method, we seek parameters ($a,\ b$) in eq. (4) or k in eq. (5) that produces a maximum RMS ratios for GRACE estimated mass fields.

For chosen values of the parameters (a, b) or k, degree and order dependent weights from eq. (4) or (5), in eq. (2) allows us to use eq. (3) to compute global surface mass change (in units of cm of equivalent water load change) on 1° latitude x 1° longitude grids from the 22 GRACE solutions, truncated at degree and order 60 (i.e., N = 60), and excluding the C_{20} coefficient.

Figure 2 shows RMS ratios of the 22 GRACE estimated mass fields computed for a range of parameters (*a, b*). The range for (*a, b*) was deduced from preliminary tests. A maximum RMS ratio (~ 2.19) correspond to $a = 1.6$, and $b = 2.0$. This solution ($a = 1.6$, $b = 2.0$) is deduced from the mean RMS ratio for the 22 solutions. It is possible to perform the same search for individual GRACE solutions, and the results would vary if the quality of solutions varies. The global mean RMS ratio is computed from the sum of RMS ratios at each grid point with cosine of latitude as weighting.

Similar experiments for the second method (eq. 5) are shown in Figure 3. A maximum RMS ratio (~ 2.19) can be easily identified, corresponding to a value of $k = 3.4$ for the mean of all 22 solutions. The two optimized smoothing methods (RMS and FM) produce nearly identical maximum RMS ratio (2.1931 vs. 2.1928), with the RMS method generates a slightly higher maximum value. We should point out that when the weights are computed using eq. (4) and (5), the effects of elastic deformation from terrestrial water storage and ocean bottom pressure changes are not considered. This is based on our additional experiments (not presented here) to compare the results of two cases, including or excluding the effects of elastic

deformation. When excluding the effects of elastic deformation, the two optimized smoothing methods produce consistently higher maximum RMS ratios between land and ocean. This is equivalent to an increase of weight for low degree Stokes coefficients.

Figure 4 shows similar RMS ratios when the Gaussian smoothing is used, as a function of the spatial radius. Interestingly, RMS ratios from the Gaussian smoothing reach a maximum value (~ 1.88) when the spatial radius r is 800 ~ 1000 km, very similar to the optimal value (~ 800 km) suggested by *Chen et al.* [2005a] based on minimized RMS residuals between GRACE observations and GLDAS estimates. These RMS ratio analyses indicate that using the proposed optimized smoothing can significantly improve the signal-to-noise ratio than the Gaussian smoothing (2.19 vs. 1.88) in GRACE estimate terrestrial water storage changes.

4. Water Storage Changes From the Optimized Smoothings

4.1. Assessment of the Optimized Smoothings

We compare results from the two optimized smoothing methods with water storage changes from Gaussian smoothing with an 800 km radius, a value recommended by *Chen et al.* [2005a]. The left 4 panels of Figure 5 show GRACE water storage in Apr. 2003 from (a) 800 km Gaussian smoothing, and 3 cases using the RMS-dependent smoothing (based on eq. 4). Parameters were (c) RMS Case01 is when $a = 1$ and $b = 1$, (e) RMS Case02 is when $a = 1$ and $b = 2$, and (g) RMS Case03 with optimum values $a = 1.6$ and $b = 2.0$. The right 4 panels are similar comparisons for Oct. 2003. April and October are months of maximum and minimum

storage in the seasonal global water cycle [*Wahr et al.,* 2004; *Tapley et al*., 2004b; *Chen et al*., 2005a]. With relatively large signal-to-noise levels during these months, it should be easier to identify improvements in water storage estimates.

Figure 5 shows that results are sensitive to the choice of parameters *(a, b)*. The optimized parameter case (RMS Case03) shows load changes that correspond well with land masses and river basins, and little organized variation over the oceans (e.g., in the South Atlantic, Fig. 5h). In contrast, 800 km Gaussian smoothing shows organized longitudinal stripes over the oceans. For most major river basins, amplitudes in RMS Case03 exceed those from Gaussian smoothing. We interpret this as the effect of signal attenuation (or leakage error) in Gaussian smoothing.

Figure 6 shows similar comparisons (as in Figure 5), for various scale parameters k in eq. (4): FMCase01 $k = 1$, FM Case02 $k = 10$, and FM Case03 $k = 3.4$, the optimum value. Results are sensitive to the choice of k. Residuals over the oceans from FM Case02 appear smaller than those of optimized FMCase03, but variations over the land are also smaller. In both cases, (Figures 5 and 6) using the optimized parameters provides similar results for these two months. (Apr., Oct. 2003). RMS Case03 shows slightly more details than FM Case03, e.g., in the Eurasia continent (Figs. 5g and 6g).

4.2 Equivalent Spatial Resolution

Spatial smoothing will affect estimated signal levels, and in the case of simple Gaussian smoothing, lower variance will result as the smoothing radius is increased. To quantify this, we

apply Gaussian smoothing and the two optimized smoothing methods to the same GLDAS (plus baroclinic oceanic) data for Apr. 2003 and Oct. 2003 in the left and right 4 panels of Figure 7, respectively. The top 2 panels (a, b) are for the GLDAS estimates with no smoothing, (c) and (d) for GLDAS with 500 km Gaussian smoothing, (e) and (f) for GLDAS with RMS Case03 smoothing, and (g) and (h) for GLDAS with FM Case03 smoothing. We tested Gaussian smoothing with additional radius parameters, as well. We find that the two optimized variance-dependent smoothing methods reduced signal variance by about the same amount as does 500 km Gaussian smoothing.

4.3 Comparison with Model Estimates

The optimized variance-dependent smoothing apparently improves spatial resolution, and shows larger seasonal variability in the recovered mass fields than Gaussian smoothing examples. There remain residual variations over the oceans from the optimized smoothing which may be either of geophysical origin or due to noise. GLDAS seasonal water storage changes are smaller than the three estimates from GRACE (Gaussian 800 km, RMS Case03, FM Case03). This may be partly due to the omission of groundwater effects, or underestimate of soil and snow water change in GLDAS [*Chen et al.,* 2006].

GRACE-observed residual signals over the oceans are significantly larger than model estimated baroclinic mass variations and also show less to nearly no correlation with model estimates, indicating either the oceanic residuals from GRACE are still mostly from noise, or

the ECCO baroclinic model significantly underestimates seasonal large scale oceanic mass changes. However, some of the strong oceanic residual signals, such as the dominant positive residuals (over 5 cm of equivalent water height change in a region of nearly 40° x 40°) in the South Atlantic in Oct. 2003 (Fig. 6h) are unlikely from GRACE errors.

4.4 Basin-Scale Improvements

Here we compare results for several basins in more detail, and show that spatial resolution of our optimized smoothing methods is superior to Gaussian smoothing, in that load changes are aligned with known geographical boundaries. Figure 8 shows GRACE water storage changes Apr. 2003 in Alaska and western Canada (Yukon and Fraser basins and surrounding areas) from 800 km Gaussian smoothing (a - top panel), and RMS Case03 smoothing (b - bottom panel). The peak value with Gaussian smoothing is between 6 and 7 cm equivalent water thickness, compared to 10 to 11 cm in the RMS Case03. The boundary of the RMS Case03 aligns much better with the coast line.

The 4 panels of Figure 9 show GRACE water storage changes in South America for Apr. and Oct. 2003. The top 2 panels show 800 km Gaussian smoothing, and the bottom 2 panels show RMS Case03. In the Amazon basin, the magnitude of the seasonal signal and the large size of the basin allow 800 km Gaussian smoothing to produce estimates similar to RMS Case03. However, RMS Case03 results align better with stream lines and appear to have lower levels of variance leakage outside the basin. RMS Case03 shows larger seasonal variability, as

well. A time series comparison of water storage changes in the Amazon basin in Figure 10 shows this more clearly. As shown in Figure 9, in the Orinoco basin, a small basin north of Amazon, RMS Case03 appears to be superior relative to Gaussian smoothing, showing a load change clearly aligned with the geographical boundaries of the basin. The boundary between Amazon and Orinoco basins is also much clearer with RMS Case03, relative to Gaussian smoothing.

5. Conclusion and Discussion

The optimized variance-dependent smoothing methods appear to more effectively recover global surface mass changes from GRACE time-variable gravity measurements, when compared with Gaussian smoothing. These methods maximize the variance ratio of mass changes over the land relative to those over the ocean. They produce lower levels of variance leakage associated with a finite range of spherical harmonics, and improved spatial resolution, as measured by the coincidence of water loads with known geographical boundaries.

These two methods assign degree-and-order dependent weights to Stokes coefficients using information from the GLDAS land surface modeling system and baroclinic oceanic residuals estimated from models [Wahr et al., 2004]. In one case, the weight is a ratio between model RMS and GRACE RMS, to make the GRACE spherical harmonic spectrum more similar to that of model estimate. Adjustable parameters are chosen to maximize the mean variance ratios of mass changes over the land relative to those over the ocean. The second

methods follows a least squares criterion where the weight is the sum of signal (GLDAS + barotropic ocean) over signal plus noise variance, with an adjustable scaling parameter, again chosen to maximize the variance ratio of mass changes over the land relative to those over the ocean. These two methods show similar results, although RMS Case03 appears to have slightly better signal-to-noise levels relative to FM Case03 smoothing. These methods also appear to be better than the dynamic basin function results of *Seo and Wilson* [2005], especially for smaller basins [*Seo et al*., 2006]. The improvements over the order-depending smoothing results of *Han et al.* [2005a] are also evident.

From a philosophical point of view, one might be concerned about the dependence of the weights on the land surface and oceanic models. Since only the mean RMS variability of the model estimates are employed, any good land surface model can be used, with probably similar results. The main point is that the land surface model has imbedded in it the geographical information about river basins locations, and regions where signal variance is expected to be concentrated. Using degree and order dependent weights based on the model spectrum forces the GRACE results to have similar geographical behavior. As an improvement on this method, we can add additional features to GLDAS mass variations, to allow for other components of surface mass change that should be in GRACE, but are not in GLDAS. One of these is certainly the variations over Greenland and Antarctica, and there are at least seasonal models of these that could be added to GLDAS.

Additional experiments from this study indicate that when elastic deformation from water storage and ocean bottom pressure changes is not considered, these two optimized smoothing methods produce relatively higher maximum RMS ratio. Any method that suppresses high degree and order terms will reduce signal as well as noise, and a restoring method such as that discussed by *Chen et al.* [2005d] would be appropriate to correct for this effect.

Acknowledgments. We would like to thank John Wahr and an anonymous reviewer for their insightful comments, which led to improved presentations of the results. We are especially grateful to John Wahr for providing the Stokes coefficients computed from the ECCO and a barotropic ocean general circulation models. This research was supported by NASA's Solid Earth and Natural Hazards and GRACE Science Program (under Grants NNG04GF10G, NNG04GF22G, NNG04GE99G).

References:

Bettadpur, S. (2003), Level-2 Gravity Field Product User Handbook, The GRACE Project.

Chambers, D.P., J. Wahr, and R. S. Nerem (2004), Preliminary observations of global ocean mass variations with GRACE, Geophys. Res. Lett., 31, L13310, doi:10.1029/2004GL020461.

Chao, B.F., and R.S. Gross (1987), Changes in the Earth's rotation and low-degree gravitational field introduced by earthquakes, Geophy. J. R. Astron. Soc., 91, 569-596.

Chen, J.L., C.R. Wilson, R.J. Eanes, and R.S. Nerem (1999), Geophysical Interpretation of Observed Geocenter Variations, J. Geophy. Res., Vol. 104, No. B2, 2683 - 2690.

Chen, J.L., C.R. Wilson, Low Degree Gravitational Changes from Earth Rotation and Geophysical Models, Geophy. Res. Lett., Vol. 30, No. 24, 2257, doi:10.1029/2003GL018688, 2003.

Chen, J.L., C.R. Wilson, B.D. Tapley (2004), Low Degree Gravitational Changes from GRACE: Validation and Interpretation, Geophys. Res. Lett., Vol. 31, No. 22, L22607 10.1029/2004GL021670.

Chen, J.L., C.R. Wilson, J. S. Famiglietti, and M. Rodell (2005a), Spatial Sensitivity of GRACE Time-Variable Gravity Observations, J. Geophys. Res., 110, B08408, doi:10.1029 /2004JB003536.

Chen, J.L., M. Rodell, C.R. Wilson, J. S. Famiglietti (2005b), Low Degree Spherical Harmonic Influences on GRACE Water Storage Estimates, Geophys. Res. Lett., Vol. 32, No. 14, L14405 10.1029/2005GL022964.

Chen, J.L., C.R. Wilson, B.D. Tapley, J. S. Famiglietti, and M. Rodell (2005c), Seasonal Global Mean Sea Level Change From Altimeter, GRACE, and Geophysical Models, J. Geodesy DOI 10.1007/s00190-005-0005-9 ,Vol. 79, No. 9, 532 - 539.

Chen, J.L., C.R. Wilson, J. S. Famiglietti, M. Rodell, B.D. Tapley (2006), Restoring Seasonal Basin-Scale Water Storage Change From Smoothed GRACE Time-Variable Gravity, Water Resources Res. (in review).

Ek, M. B., K. E. Mitchell, Y. Lin, E. Rogers, P. Grunmann, V. Koren, G. Gayno, and J. D. Tarpley (2003), Implementation of the upgraded Noah land-surface model in the NCEP operational mesoscale Eta model, J. Geophys. Res., 108, 8851, doi:10.1029/2002JD003296.

Han, S.-C., C.K. Shum, C. Jekeli, C.-Y. Kuo, C.R. Wilson, K.-W. Seo (2005a), Non-isotropic filtering of GRACE temporal gravity for geophysical signal enhancement, Geophys. J. Int. 163, 18–25 doi: 10.1111/j.1365-246X.2005.02756.x.

Han, S.-C., Shum, C.K., Jekeli, C., Alsdorf, D. (2005b), Improved estimation of terrestrial water storage changes from GRACE, Geophys. Res. Lett., Vol. 32, No. 7, L07302 10.1029/2005GL022382.

Jekeli, C. (1981), Alternative Methods to Smooth the Earth's Gravity Field, Department of Geodetic Science and Surveying, Ohio State University, Columbus, OH.

Rodell, M., P. R. Houser, U. Jambor, J. Gottschalck, K. Mitchell, C.-J. Meng, K. Arsenault, B. Cosgrove, J. Radakovich, M. Bosilovich, J. K. Entin, J. P. Walker, D. Lohmann, and D. Toll (2004a), The Global Land Data Assimilation System, Bull. Amer. Meteor. Soc., 85 (3), 381–394.

Rodell, M., J.S. Famiglietti, J.L. Chen, S. Seneviratne, P. Viterbo, and S. Holl (2004b), River basin water budget estimates of evapotranspiration using GRACE derived terrestrial water storage with observation based precipitation and runoff, Geophys. Res. Lett., Vol. 31, No. 20, L20807, 10.1029/2004GL021104.

Seo, K.-W., C.R. Wilson (2005), Simulated estimation of hydrological loads from GRACE, J. Geodesy, Vol. 78, No. 7-8, 442 – 456.

Seo, K.-W., C.R. Wilson, J. S. Famiglietti, J.L. Chen, M. Rodell (2006), Terrestrial Water Mass Changes From GRACE, Water Resources Research (in press).

Swenson, S., and J. Wahr (2002), Methods for inferring regional surface-mass anomalies from Gravity Recovery and Climate Experiment (GRACE) measurements of time-variable gravity, J. Geophys. Res., 107(B9), 2194, doi: 0.1029/2001JB000576.

Tapley, B.D., S. Bettadpur, M.M. Watkins, C. Reigber (2004a), The Gravity Recovery and Climate Experiment; Mission Overview and Early Results, Geophy. Res. Lett., Vol. 31, No. 9, L09607, 10.1029/2004GL019920.

Tapley, B.D., S. Bettadpur, J. Ries, P.F. Thompson, and M.M. Watkins (2004b), GRACE Measurements of Mass Variability in the Earth System, Science, Vol. 305, 503-505.

Wahr, J., M. Molenaar, and F. Bryan (1998), Time-variability of the Earth's gravity field: Hydrological and oceanic effects and their possible detection using GRACE, J. Geophys. Res., 103(B12), 30,205– 30,230.

Wahr, J., S. Swenson, V. Zlotnicki, and I. Velicogna (2004), Time-Variable Gravity from GRACE: First Results, Geophy. Res. Lett., 31, L11501, doi:10.1029/2004GL019779, 2004.

Figures:

Figure 1. Mean RMS ratios between GRACE-observed (*GRC*) and model-predicted (*MLD*) time-variable Stokes coefficients. For each Stokes coefficient C_{lm} or S_{lm}, the ratio represents the mean RMS of the 22 GRACE solutions over the mean RMS of model-predictions during the same periods.

Figure 2. The mean RMS ratios between GRACE observed signals over land and noise (plus signals) over the ocean as a function of scale factors *a* and *b* as defined in eq. (3). The mean RMS ratios are computed from the mean land and ocean RMS of 22 GRACE estimated mass fields.

Figure 3. Mean RMS ratios between GRACE-observed signals over land and noise (plus signals) over the ocean as a function of scale factor *k* as defined in eq. (4). The mean RMS ratios are computed from the mean land and ocean RMS of 22 GRACE estimated mass fields.

Figure 4. . Mean RMS ratios between GRACE-observed signals over land and noise (plus signals) over the ocean as a function of the spatial radius (r) used in Gaussian smoothing. The mean RMS ratios are computed from the mean land and ocean RMS of 22 GRACE estimated mass fields.

Figure 5. The left 4 panels show GRACE estimated global terrestrial water storage changes in Apr. 2003 with (a) 800 km Gaussian smoothing, and 3 selected RMS weighted smoothing methods, (c) RMS Case01, (e) RMS Case02, and (g) RMS Case03. The right 4 panels are the same comparisons for Oct. 2003.

Figure 6. The left 4 panels show GRACE estimated global terrestrial water storage changes in Apr. 2003 with (a) 800 km Gaussian smoothing, and 3 selected formal (FM) error weighted smoothing methods, (c) FM Case01, (e) FM Case02, and (g) FM Case03. The right 4 panels are the same comparisons for Oct. 2003.

Figure 7. GLDAS estimated global terrestrial water storage changes (plus oceanic residual signals) in Apr. 2003 (the left 4 panels), and Oct. 2003 (the right 4 panels) in 4 cases, (a) and (b) without any smoothing, (c) and (d) 500 km Gaussian smoothing, (e) and (f) optimized RMS weighted smoothing (RMS Case03), and (g) and (h) optimized formal error weighted smoothing (FM Case03).

Figure 8. GRACE estimated water storage changes in the Yukon and Fraser basins (located in Alaska and western Canada) with (a) 800 km Gaussian smoothing and (b) optimized RMS weighted smoothing (RMS Case03).

Figure 9. GRACE estimated water storage changes in South America in Apr. 2003 (a and c) and Oct. 2003 (b and d) using 800 km Gaussian smoothing (a and c) and optimized RMS weighted smoothing (RMS Case03) (d and e).

Figure 10. GRACE estimated water storage change in the Amazon basin in 3 cases, RMS Case03, 800, and 1000 km Gaussian smoothing.

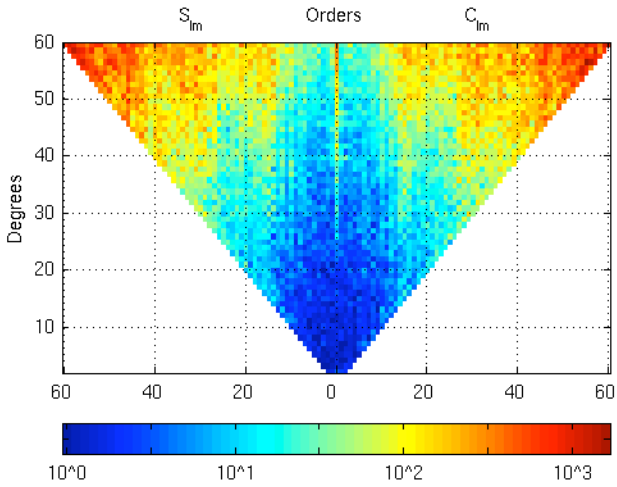

Figure1

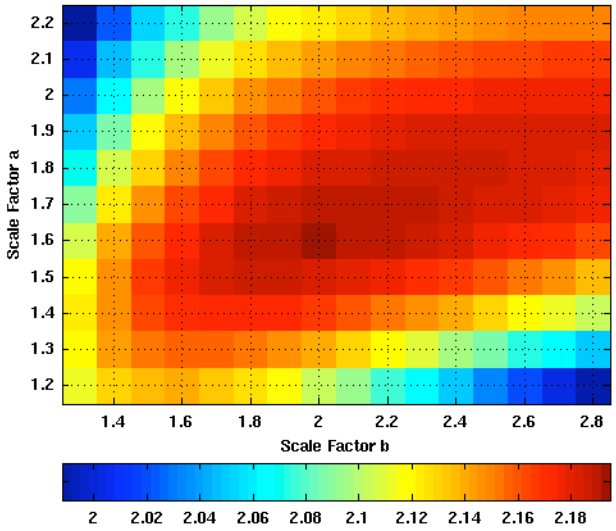

Figure 2

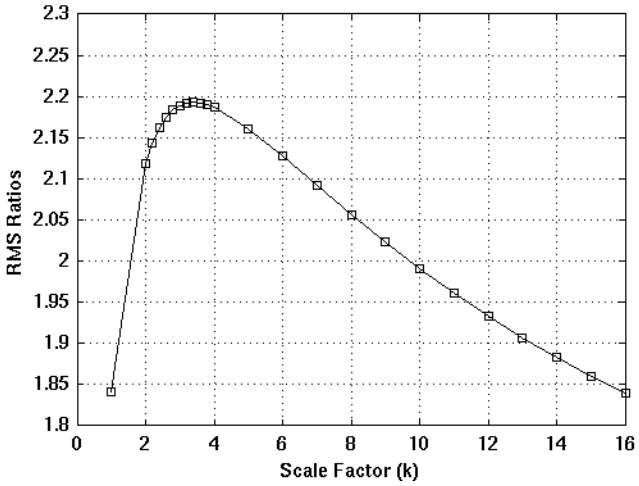

Figure 3

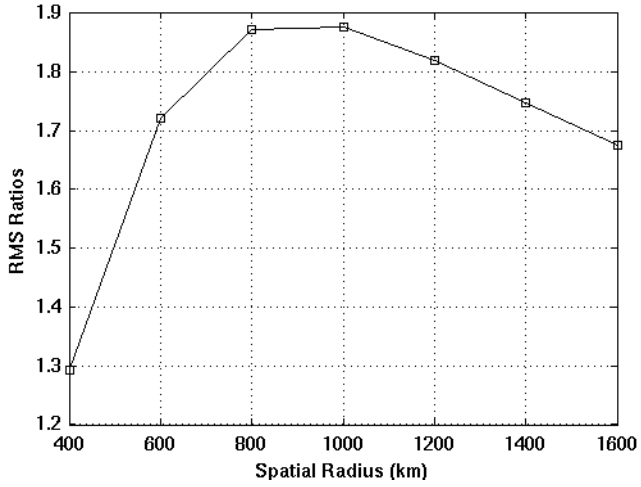

Figure 4

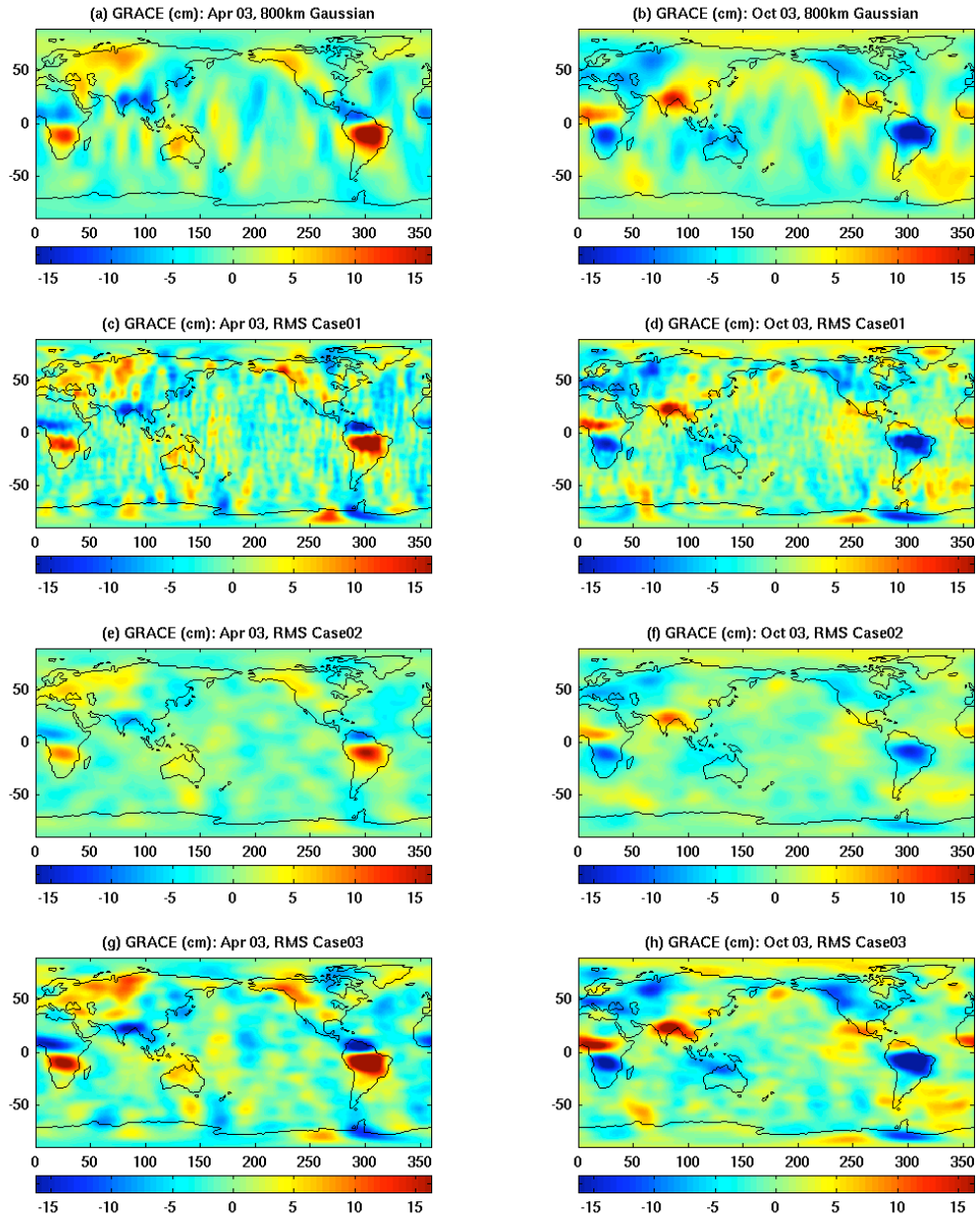
(a) GRACE (cm): Apr 03, 800km Gaussian
(b) GRACE (cm): Oct 03, 800km Gaussian
(c) GRACE (cm): Apr 03, RMS Case01
(d) GRACE (cm): Oct 03, RMS Case01
(e) GRACE (cm): Apr 03, RMS Case02
(f) GRACE (cm): Oct 03, RMS Case02
(g) GRACE (cm): Apr 03, RMS Case03
(h) GRACE (cm): Oct 03, RMS Case03
50
0
-50
0 50 100 150 200 250 300 350
-15 -10 -5 0 5 10 15

Figure 5

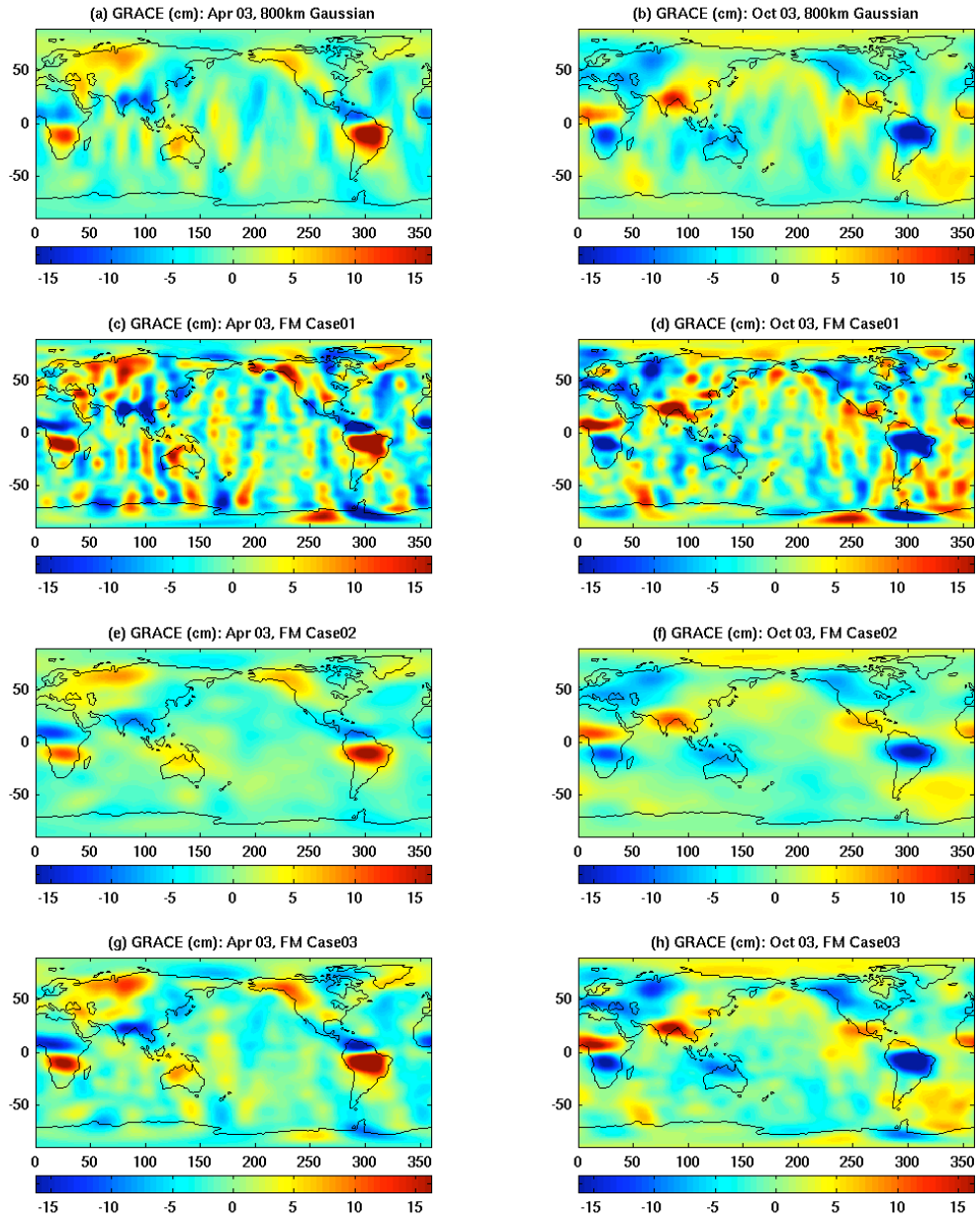
(a) GRACE (cm): Apr 03, 800km Gaussian
(b) GRACE (cm): Oct 03, 800km Gaussian
(c) GRACE (cm): Apr 03, FM Case01
(d) GRACE (cm): Oct 03, FM Case01
(e) GRACE (cm): Apr 03, FM Case02
(f) GRACE (cm): Oct 03, FM Case02
(g) GRACE (cm): Apr 03, FM Case03
(h) GRACE (cm): Oct 03, FM Case03
50
0
-50
0 50 100 150 200 250 300 350
-15 -10 -5 0 5 10 15

Figure 6

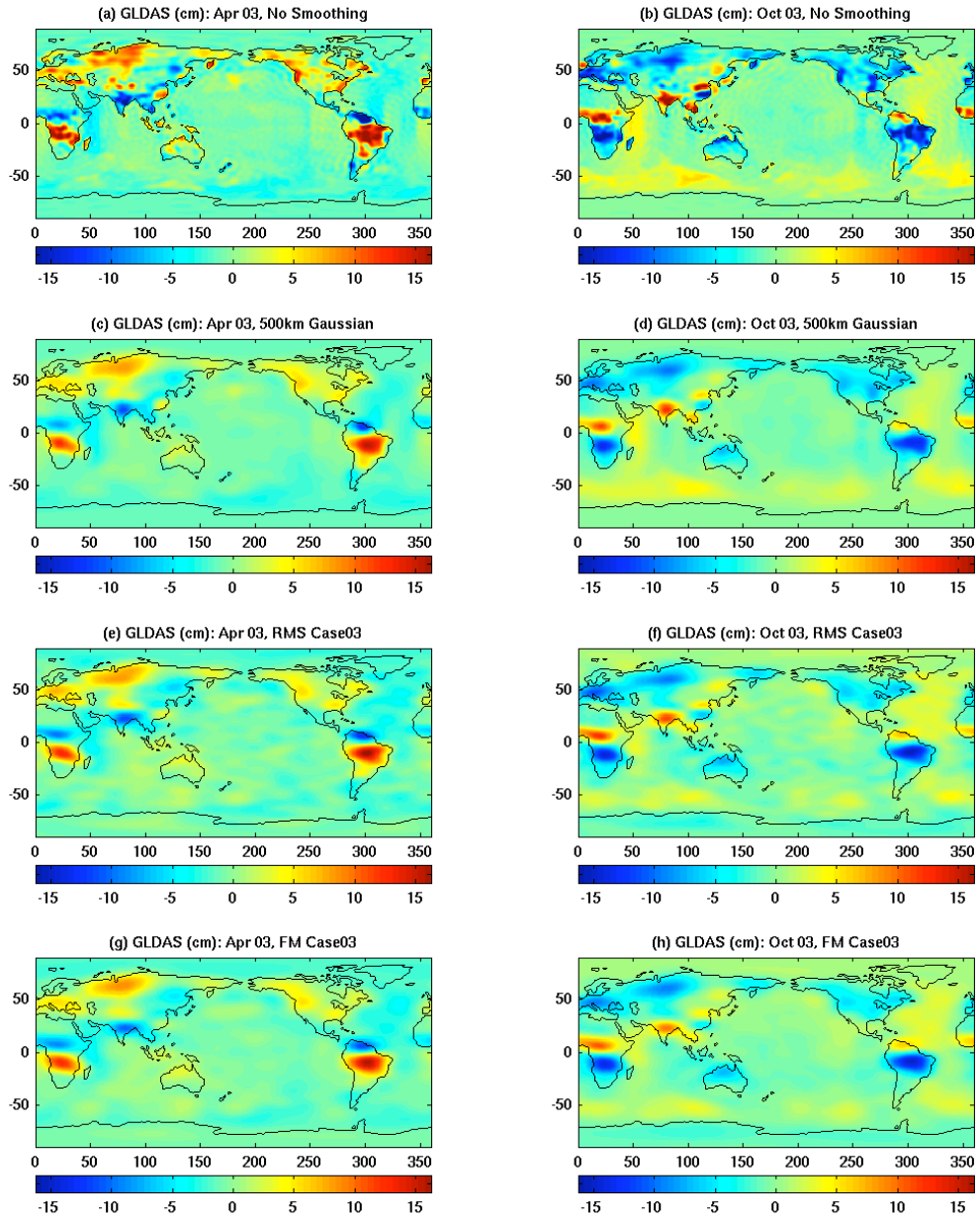
(a) GLDAS (cm): Apr 03, No Smoothing
(b) GLDAS (cm): Oct 03, No Smoothing
(c) GLDAS (cm): Apr 03, 500km Gaussian
(d) GLDAS (cm): Oct 03, 500km Gaussian
(e) GLDAS (cm): Apr 03, RMS Case03
(f) GLDAS (cm): Oct 03, RMS Case03
(g) GLDAS (cm): Apr 03, FM Case03
(h) GLDAS (cm): Oct 03, FM Case03
50
0
-50
0 50 100 150 200 250 300 350
-15 -10 -5 0 5 10 15

Figure 7

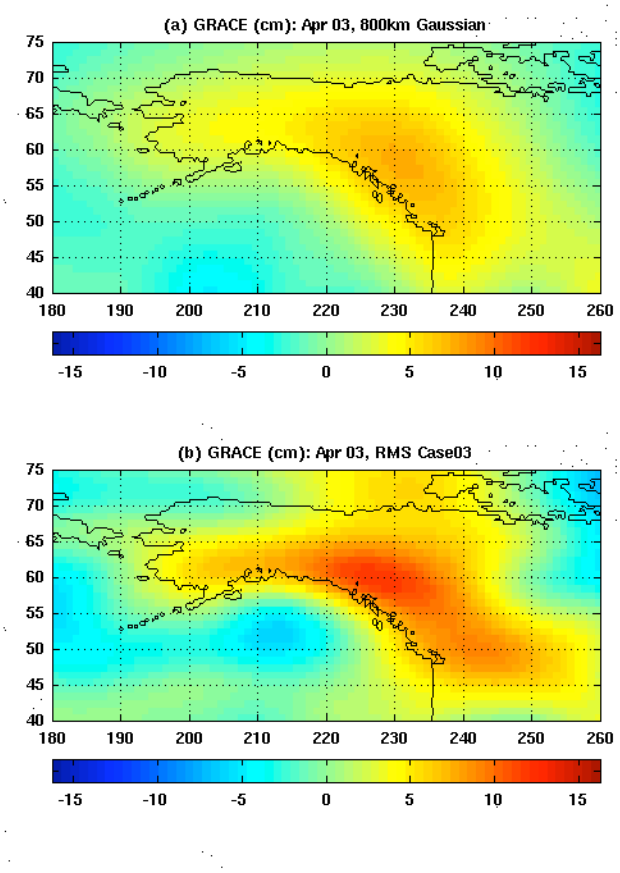
(a) GRACE (cm): Apr 03, 800km Gaussian
75
70
65
60
55
50
45
40
180
190
200
210
220
230
240
250
260
-15
-10
-5
0
5
10
15
(b) GRACE (cm): Apr 03, RMS Case03
75
70
65
60
55
50
45
40
180
190
200
210
220
230
240
250
260
-15
-10
-5
0
5
10
15

Figure 8

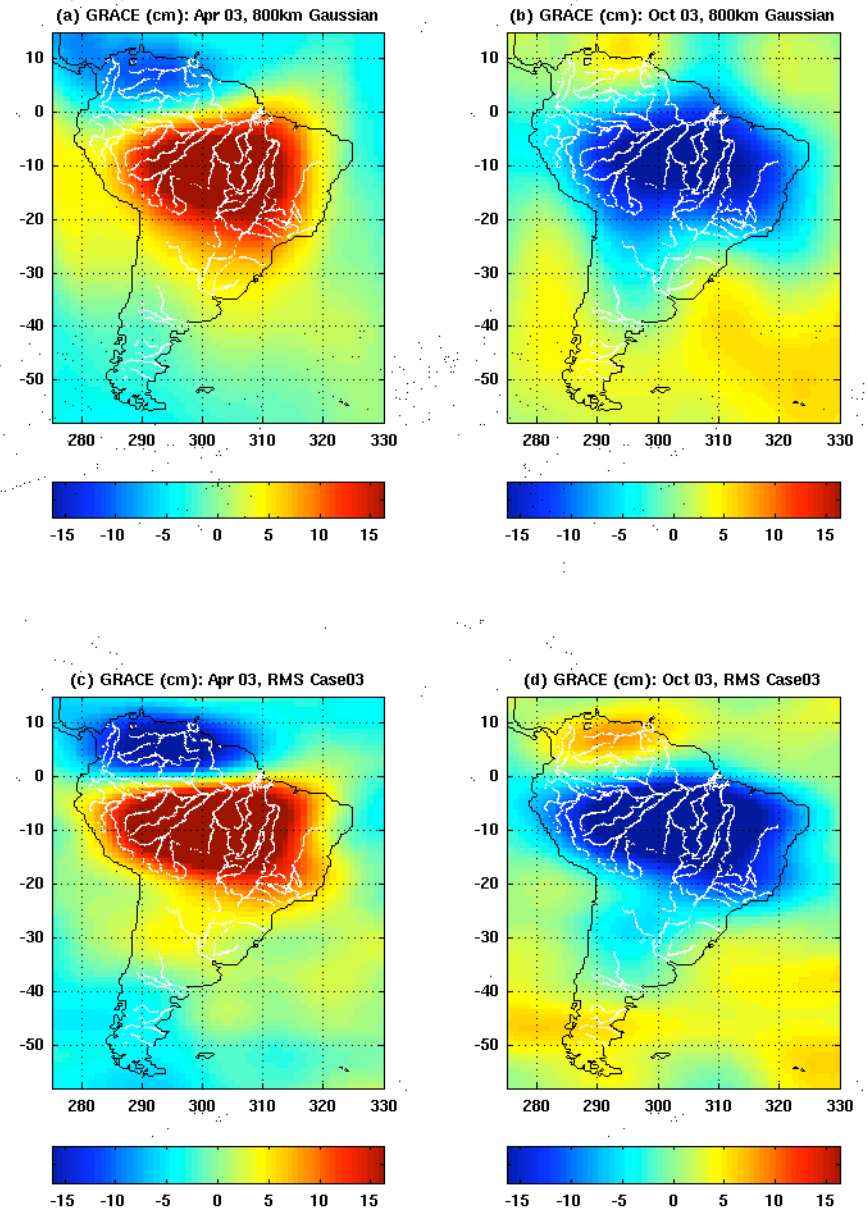
(a) GRACE (cm): Apr 03, 800km Gaussian
(b) GRACE (cm): Oct 03, 800km Gaussian
(c) GRACE (cm): Apr 03, RMS Case03
(d) GRACE (cm): Oct 03, RMS Case03
10
0
-10
-20
-30
-40
-50
280
290
300
310
320
330
-15
-10
-5
0
5
10
15

Figure 9

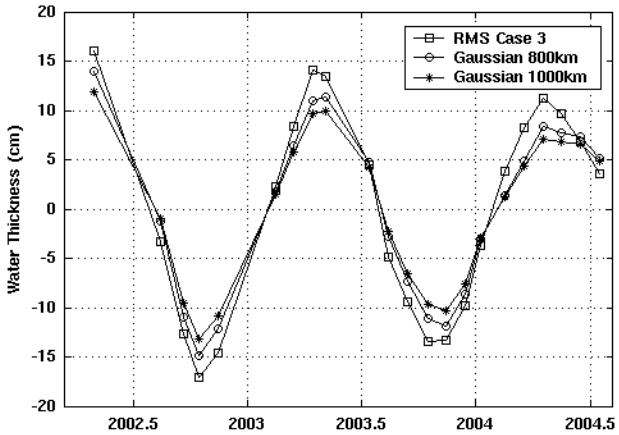
RMS Case 3
Gaussian 800km
Gaussian 1000km
Water Thickness (cm)
20
15
10
5
0
-5
-10
-15
-20
2002.5
2003
2003.5
2004
2004.5

Figure 10